

Stress corrosion cracking of Al–Mg–Zn–Cu alloys after precompression

REINHOLD HERMANN

Faculty of Technology, The Open University, Milton Keynes, England, UK

Stress corrosion cracking (SCC) experiments have been carried out on double-cantilever-beam (DCB) specimens of 7017-T651 aluminium alloy. The specimens were first subjected to a known compressive load which caused plastic deformation at the notch tip. On unloading, this region developed a residual tensile stress field and on subsequent exposure to moist air at 40° C (95% relative humidity, r.h.), intergranular cracks formed. These cracks grew at a decelerating rate until they stopped. The final crack length increased with the value of the initial compressive preload, provided this was below the value for general yielding of the alloy. Electron fractography has been used to correlate changes in surface morphology with crack growth rate. It was found that ductile tearing of the notch tip may occur during unloading when the compression exceeds – 30 kN. The practical importance of these results is outlined.

1. Introduction

Stress corrosion cracking (SCC) of high strength aluminium alloys has been investigated extensively [1–5]. In the majority of these cases, the effect of changes in the environment and external load application has been studied. These studies have normally reported the dependence of SCC growth rate on both exposure time and stress intensity for a given crack environment. The results from an investigation by Finnegan and Hartt [1] on double-cantilever-beam (DCB) specimens of 7079-T651 alloys indicated that there is no unique relationship between stress intensity and crack growth rate, although the crack growth rate varied inversely with exposure time for the early part of this experiment.

Haynie [2] reported that atmospheric levels of sulphur dioxide on 7005-T53 alloy induced stress-accelerated intergranular corrosion cracking, but varying levels of other gases caused little damage at constant stress levels.

Constant strain rate techniques as used by Payer, Berry and Body [4] were employed to assess the susceptibility of metals and alloys to SCC. Stress-corrosion failure occurred either in a ductile or brittle manner depending on the

environment. Several parameters were suggested to describe the extent of SCC for a variety of environments.

In the above experiments the specimens were preloaded in tension.

However, recent experiments on compressively preloaded compact tension specimens made of medium carbon steel have shown that stage II fatigue cracks can nucleate and grow under cyclic compressive loads provided the specimens contain a sufficient level of residual tensile stress [6].

In most cases it is accepted that a tensile stress is necessary in order to get SCC and this has been obtained by applying an external load. However, tensile residual stresses can be induced by compressive loading. Such conditions can occur during manufacture and handling and are more difficult to monitor.

In order to study the effects of such stresses sharply notched test pieces of the commercial alloy 7017-T651 (which is used for armour plate) have been deliberately loaded in compression. This gives rise to a residual tensile stress ahead of a crack tip after the load has been removed.

This paper describes SCC in the presence of such residual tensile stresses.

TABLE I Chemical analysis in wt% of 7017-T651 alloy plate

Cu	Mn	Mg	Fe	Si	Zn	Ti	Cr	Zr	Al
0.11	0.29	2.30	0.35	0.18	4.78	0.04	0.15	0.14	balance

TABLE II Crack profile dimensions for SCC specimen

Compressive preload (kN)	Crack length at surface		Crack length at centre after 1000 h (mm)	Crack length differential after 1000 h (mm)
	After 200 h (mm)	After 1000 h (mm)		
-10	0.05	0.60	1.19	0.59
-20	0.60	1.03	1.86	0.83
-30	0.95	1.35	2.11	0.76
-40	3.0	3.14	3.25	0.11
-50	4.0	4.47	3.54	-0.93

2. Experimental details

The chemical analysis of 7017-T651 is given in Table I. The microstructure of the "as-received" material is shown in Fig. 1. The section is taken perpendicular to the rolling plane revealing an elongated fibrous microstructure typical of cold rolled aluminium alloys.

The present experiments employed (DCB) specimens cut from a 400 mm × 200 mm × 30 mm plate of 7071-T651 alloy; specimens had a sharp V-notch cut parallel to the rolling plane and had the following dimensions: length (*L*) 98 mm, height (*2h*) 30 mm and thickness (*B*) 25 mm. A diagram is presented in Fig. 2. A series of five specimens was preloaded compressively in a servo-hydraulic testing machine between -10 and -50 kN. After unloading, the specimens were transferred to a humidity cabinet containing a tray of distilled water. This gave a relative humidity of 95% when the temperature was



Figure 1 Polished and etched section of 7017-T651 plate perpendicular to rolling plane revealing highly banded structure with inclusions. The rolling direction is from left to right.

40° C. Incremental crack measurements were made at 10 min intervals in the first hour, every 15 min between 1 and 2 h and every hour between 2 and 8 h. Subsequently crack length measurements every 25 h were recorded up to 1000 h of exposure. All crack measurements were carried out on the specimen surface with an optical travelling microscope. The instrument was placed against the glass door of the humidity cabinet and the readings were obtained without removing the specimens from the cabinet. The accuracy of the microscope readings was estimated to be ± 0.02 mm.

A tensile load was then applied to each specimen to break it open and the fracture surfaces were examined in the scanning electron microscope (SEM).

Values for the stress intensity K_I of cracked DCB test pieces were computed by using the expression of Rippling *et al.* [5]

$$K_I = \frac{vEh}{4} \frac{[3h(a + 0.6h)^2 + h^3]^{\frac{1}{2}}}{(a + 0.6)^3 + h^2a} \quad (1)$$

where *v* is the crack opening displacement, *E* is Young's modulus, *a* is crack length and *h* is the height of the specimen. The relationship between K_I and the crack velocity under ambient laboratory conditions was investigated by Alcan Laboratories Ltd [7] and appears in the next section.

3. Results and discussion

3.1. Crack growth data

In Table II a summary of the final crack profile dimensions for a relative humidity of 95% is presented. From this table the following points can be made:

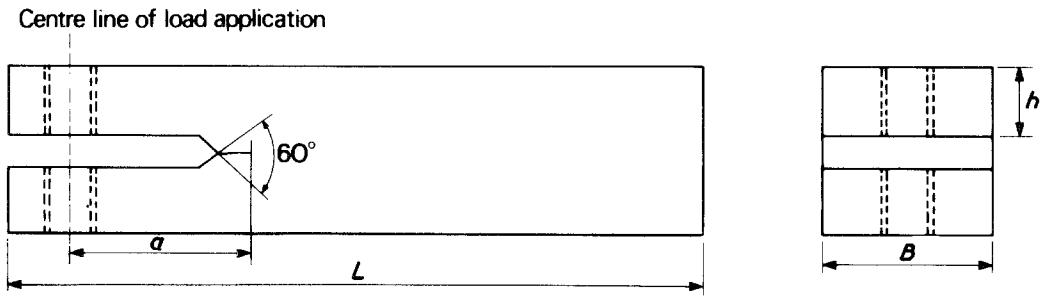


Figure 2 Geometry of 7017-T651 aluminium alloy test specimen.

3.1.1. Effect on preload

Most crack growth occurs in the first 200h of exposure for specimens preloaded between -30 and -50 kN. Crack growth then decelerates until arrest occurs. After 1000h the crack length on the surface is different from that at the centre of the same specimen. This is thought to be a consequence of the fact that the plastic zone size (and hence the residual stress zone size) is larger at the surface than at the centre of the section.

3.1.2. Crack morphology

The marked variation in crack surface appearance is shown in Fig. 3. The first three specimens (marked 1 to 3) show a convex crack front, while 4 and 5 are clearly concave with some reverse bowing towards the edge of the specimen. On these two specimens and specimen 3, three distinct regions are visible; the grey fracture just above the notch region "a" has the same appearance as the "break open" fracture at the top of region "c". Between these two similar areas lies a light region of SCC, region "b". More detail is given in Fig. 4, which is a magnified view of the fracture surface of the -50 kN preloaded specimen.

Fig. 5 shows the relationship between final crack length and compressive preload. The total crack length as measured at the edge of the specimen, displays a very steep curve, in contrast

to the length of the stress corrosion crack whose curve approximates to a straight line.

Fractographic examination in the SEM confirms that the fracture appearance next to the notch for specimens preloaded at -30 to -50 kN is identical to the "break open" fracture. The SCC fracture surface is shown in Fig. 6a and is predominantly intergranular. The boundary between a stress corrosion fracture surface and the subsequent "break open" fracture for the specimen preloaded at -30 kN is shown in Fig. 6b.

For preloads ranging from -30 to -50 kN some ductile tearing occurs from the notch tip during unloading thereby nucleating a crack which can grow subsequently by stress corrosion cracking. This ductile rupture surface exhibits some interesting features. Fig. 7 shows an example of a crack formed on unloading a specimen. Within a few minutes of unloading a crack forms along a line of inclusions, suggesting that ductile tearing occurs at the interface between precipitates or inclusions and the metal.

A second experiment was carried out in which a specimen was preloaded in air to -45 kN and then immediately transferred to a vacuum chamber. Cracks were sought immediately after unloading and after spending 350h in a vacuum at 10^{-3} torr. No measureable SCC was found after the specimen was broken open and examined in the SEM.

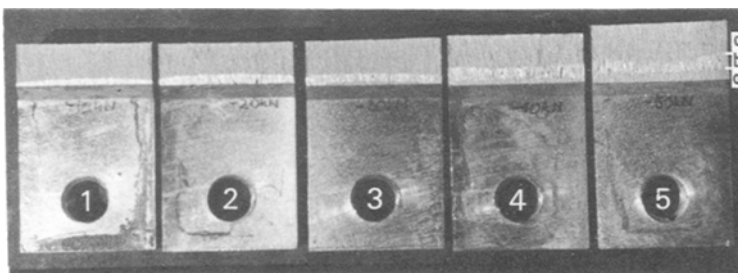


Figure 3 SC crack profiles of specimens preloaded (from left to right, respectively) to -10 , -20 , -30 , -40 and -50 kN, prior to exposure to air for 1000 h at 95% r.h.

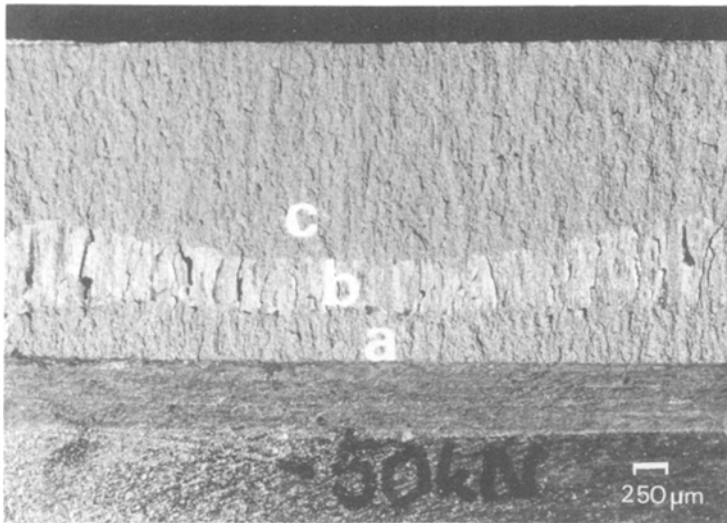


Figure 4 Fracture morphology of SC specimen subjected to -50 kN preload. Apart from the notch at the bottom, three distinct morphologies are observed; the SCC at the centre appears as a smooth surface.

3.2. Crack velocity characteristics and stress intensity correlation

In Fig. 8 the relationship between crack length and exposure time for all specimens is plotted. Together with Table II, this indicates that most crack growth appears in the first 200h of exposure time. At any point on these curves the crack growth velocity can be determined by measuring the slope of the tangent of the curve. The values of velocity shown in Table III are superimposed onto the appropriate $V-K$ curve in Fig. 9a and a number of inferred stress intensity values can be obtained. Specimens with preloads of -30 to -50 kN show a high initial crack growth rate of $10^{-7}\text{ m sec}^{-1}$ within region II of Fig. 9a in

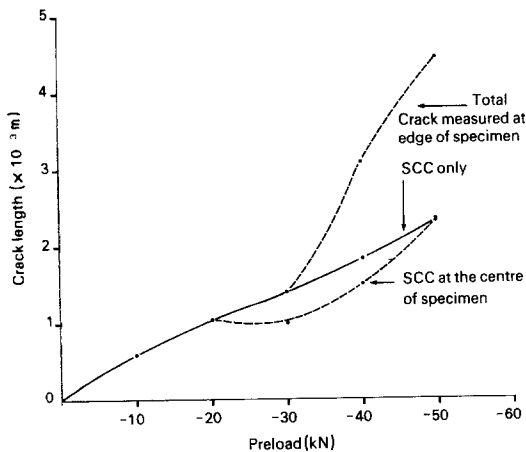


Figure 5 Crack length against compressive preload after 1000 h of exposure at 95% r.h.

which the crack growth rate is independent of the stress intensity for this alloy.

In the present stress corrosion work, inferred values of the stress intensity have been determined by the technique described above. The plateau of region II in Fig. 9a has been curtailed at $K = 15\text{ MNm}^{-3/2}$ because intensity values are accurate only for velocities below $10^{-9}\text{ m sec}^{-1}$ and for

TABLE III Inferred stress intensity values obtained by superimposing crack velocities for various preloads onto the $V-K$ curve of Fig. 9a

Preload (kN)	Crack length (mm)	Velocity (m sec^{-1})	Inferred stress intensity K_I ($\text{MNm}^{-3/2}$)
-10	0.07	4.9×10^{-9}	20
	0.28	2.9×10^{-9}	5.55
	0.70	1.1×10^{-10}	5.50
-20	0.19	1.35×10^{-8}	25
	0.50	1.22×10^{-9}	7.0
	0.94	5.1×10^{-10}	5.57
-30	1.05	1.2×10^{-10}	5.50
	0.25	1.53×10^{-8}	30
	0.90	2.38×10^{-9}	15.00
-40	1.30	2.8×10^{-10}	5.55
	1.33	1.7×10^{-11}	5.42
	1.40	1.3×10^{-7}	30
-50	2.80	3.5×10^{-9}	20
	3.02	7.6×10^{-10}	6.2
	3.14	1.1×10^{-10}	5.45
-50	1.80	1.7×10^{-7}	30
	3.80	5.0×10^{-9}	20
	4.13	2.4×10^{-10}	5.52
	4.47	1.8×10^{-10}	5.50

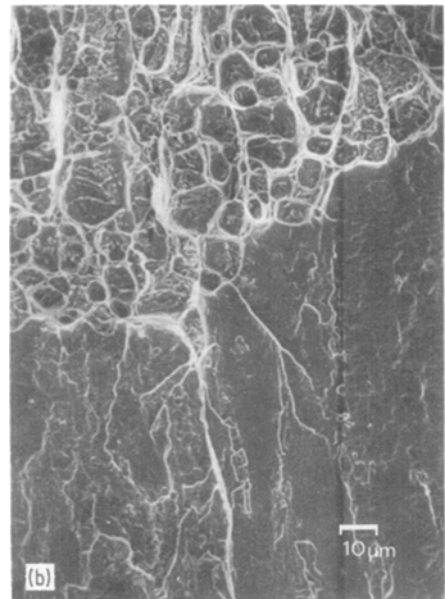
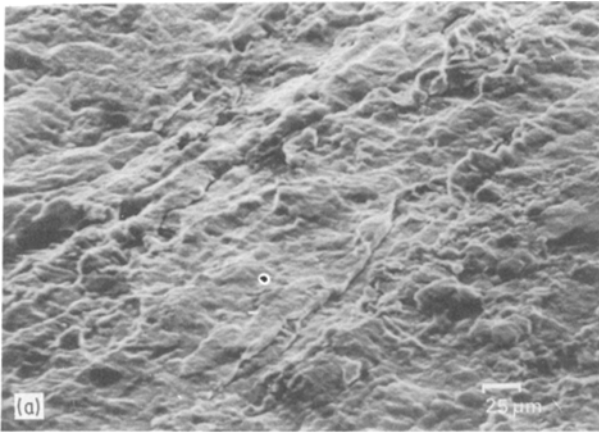


Figure 6 (a) SEM photograph of stress corroded fracture surface and (b) SEM photograph showing smooth stress corroded fracture surface on the bottom and “break open” fracture on the top.

this reason some K_I values in Table III are approximate.

In Fig. 9b inferred values of the stress intensity for preloads of -30 to -50 kN are plotted against crack length at the edge of the specimens. Each curve is displaced from the others but shows similar shapes for stress intensities between 6 and $15 \text{ MNm}^{-3/2}$. In this investigation crack growth eventually stopped at a stress intensity of about $5.5 \text{ MNm}^{-3/2}$.

In a practical application such cracks should not be disregarded, especially if the component is subjected to a subsequent tensile loading. Further crack growth may occur by either critical or subcritical modes.

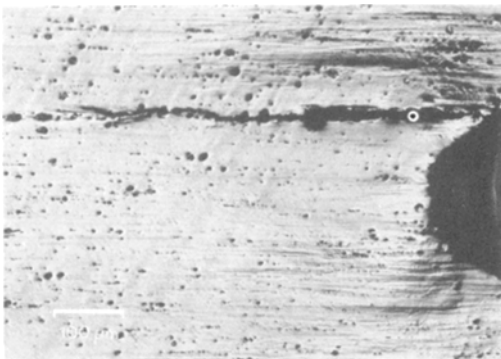


Figure 7 The specimen after application of -45 kN preload and unloading. The crack developed within 3 min after unloading following a parallel line of inclusion. Also note heavily distorted surface around the notch and slip bands that lie at approximately 45° to the crack.

4. Conclusions

(1) Compressively preloaded V-notch specimens of 7017-T651 alloy show stress corrosion cracking in an air environment of 95% r.h. The cracks grow at a decelerating rate and finally stop. The final crack length increases with the value of the initial preload.

(2) Three quarters of the total crack growth occurs in the first 200 h of exposure time, and for preloads of -30 to -50 kN the initial crack growth is independent of the stress intensity i.e. it occurs in region II of the $V-K$ curve. Above 200 h of exposure time slower region I crack growth occurs.

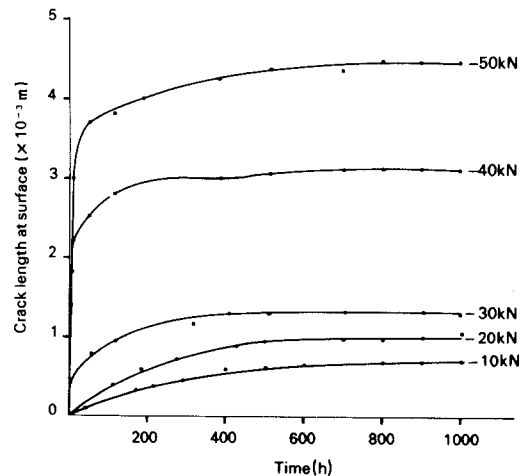


Figure 8 Crack length against time for specimens preloaded between -10 and -50 kN.

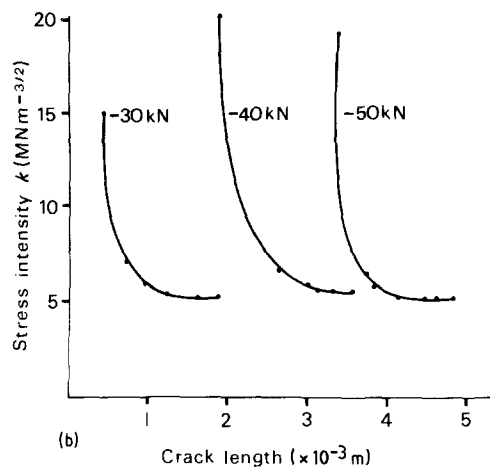
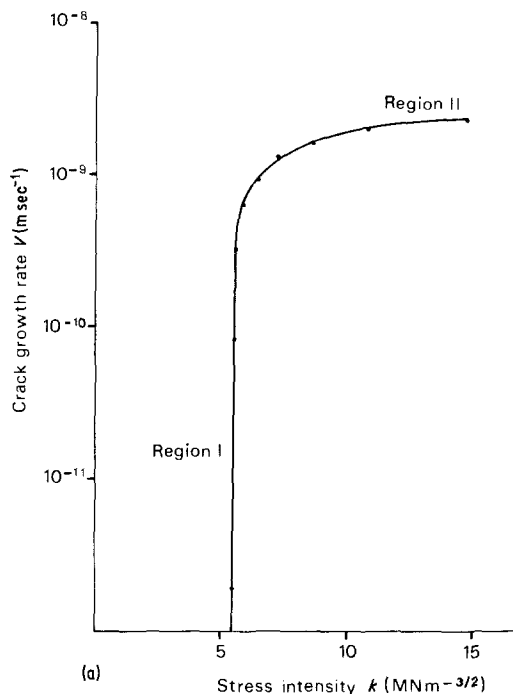


Figure 9 (a) Crack growth rate against stress intensity for 7017-T651 plate showing region I and one part of the plateau of region II and (b) stress intensity values are plotted against crack length for preloads of -30 to -50 kN.

(3) Fractography indicates: (a) that SCC is predominantly intergranular; (b) that at compressive preloads of -30 kN and above there occurs some ductile tearing during the release of the preload. These cracks subsequently grow by SCC.

(4) Up to 350h after preloading to -45 kN and unloading no SCC is observed if the specimen is kept in a vacuum of 10^{-3} torr.

Acknowledgements

The author wishes to express his thanks for help given in this work by Mr A. T. Thomas of Alcan Laboratories Ltd, Banbury, who provided the alloy plate and freely gave advice. Practical assistance was given by J. Moffatt of the Open University. Thanks must also be paid to Dr C. N. Reid and Dr J. Wood for their continuing interest in

this work and for critically reviewing the manuscript.

References

1. J. E. FINNEGAN and W. H. HARTT, ASTM-Stress Corrosion - New Approaches STP 610 (American Society for Testing and Materials, Philadelphia, 1975) pp. 44-60.
2. F. T. HAYNIE, *ibid.* pp. 32-43.
3. W. G. CLARK, Jr and J. D. LANDES, *ibid.* pp. 108-27.
4. G. H. PAYER, W. E. BERRY and W. K. BOYD, *ibid.* pp. 82-93.
5. E. J. RIPPLING, S. MOSTOVOY and R. L. PATRICK, *Mater. Res. Stand.* 4 (1964) 129.
6. C. N. REID, K. WILLIAMS and R. HERMANN, "Fatigue of Engineering Materials and Structures", Vol. 1, (Pergamon Press, Oxford, 1979) pp. 267-70.
7. R. J. DURHAM, Alcan Laboratories Ltd., Atlantic Region Research Centre, Banbury, Oxon. Private Communication, 1979.

Received 26 June 1980 and accepted 11 February 1981.